Stanford Exploration Project, Report 115, May 22, 2004, pages 467–479

Electric fields created at the seismic source - a new electroseismic phenomenon

Seth Haines[1]

ABSTRACT

Electroseismic data may show two different forms of source-related energy. The first is the electroseismic direct field which is produced at any impact source. It is approximately an electric dipole created by the asymmetrical pressure field of the impact. The second field is the electric field created by the impact of a mass on a metal hammer plate. The impact moves the hammer plate within the earth's magnetic field, and creates an electric field described by Lorentz's equation. Both show no moveout, and the amplitude pattern of a dipole. The direct field may be differentiated from the Lorentz field, however, by its reversed polarity on opposite sides of the shot point.

INTRODUCTION

Electroseismic phenomena have been shown to produce two forms of energy: the interface response and the coseismic field (Butler et al., 1996; Garambois and Dietrichz, 2001; Haines and Guitton, 2002). As explained in detail by Pride and Haartsen (1996), these phenomena depend on the pressure-induced flow of pore fluid relative to the grain matrix as a P-wave passes through a fluid-saturated porous medium. The pore fluid carries with it a small amount of electric charge due to the electric double layer that exists at the grain/fluid boundary. This mechanism produces an electric charge separation within the P-wave. The associated electric field is termed the "coseismic field". When the P-wave encounters an interface in mechanical or elastic properties, the charge distribution is disrupted and made asymmetrical; this results in what can be approximated as an oscillating disk of electric dipoles at the first Fresnel zone. The corresponding electric field is termed the "interface response" and can be observed at the Earth's surface or other remote location. It shows reversed polarity on opposite sides of the shot point, virtually zero moveout ($V_{em} >> V_p$), and the amplitude pattern of a dipole.

A third type of electroseismic energy is predicted by Equation 144 of (Pride and Haartsen, 1996):

$$E_x = T^F_{E,s_{em}} \left(\frac{i}{\omega s_{em} x} - \frac{1}{(\omega s_{em} x)^2} \right) \frac{e^{i\omega s_{em} x}}{4\pi x} 6 \cos\theta \sin\theta F \tag{1}$$

[1]**email:** shaines@pangea.stanford.edu

where

$$T^F_{E,s_{em}} = \frac{i\omega\mu\rho_f L}{G(s^2_{em} - s^2_s)} \tag{2}$$

(with original typographic error corrected). It was first reported in the literature by Haines et al. (2004). We refer to this form of electroseismic energy as the "direct field" because it is analogous to the seismic direct wave. The direct field is the electric field of a vertical electric dipole created at the location of an impact source (Figure 1). The impact source (a sledgehammer strike, for instance) creates an asymmetric fluid-pressure distribution (enhanced pressure beneath the source and decreased pressure above) which results in a similarly asymmetrical charge distribution. This charge distribution has a strong vertical dipole component, so the measured field shows reversed polarity on opposite sides of the shot point and the amplitude pattern of a dipole. The dipole is localized at the shot point and begins at the time of the source impulse and continues until the earth has relaxed to its original state.

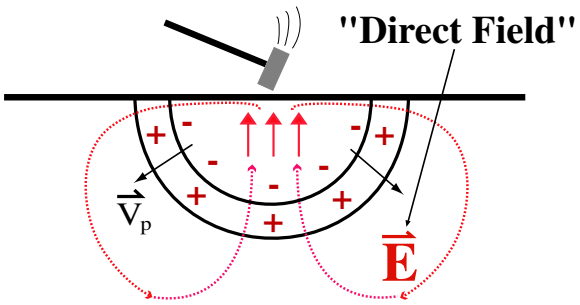

Figure 1: Cartoon diagram of the electroseismic direct field, created at the location of an impact source. shaines1-direct_field [NR]

Electroseismic data may also demonstrate the existence of a similar-looking, but entirely unrelated, electric field. This is the field of a conductor moving with velocity **v** within the Earth's magnetic field **B**, described by Lorentz's equation:

$$\mathbf{E} = \mathbf{v} \times \mathbf{B}. \tag{3}$$

If a metal hammer plate is in good electrical contact with the soil then the electric field resulting from the hammer impact may be observed at nearby electrode dipoles during the time that the hammer plate is moving, typically not more than 10 ms. The field can often be discriminated from electroseismic fields by the fact that it shows non-reversed polarity on the two sides of the shot point.

In this contribution we provide a detailed analysis of these observations and further examples of them from recently-acquired field data.

QUALITATIVE OBSERVATIONS

In orer to develop our understanding of the source-related electric fields that may be observed in electroseismic data, we begin with the simplest possible data collection scenario, and add complexity one step at a time. In this way we can better identify the impact of each individual element of electroseismic data collection.

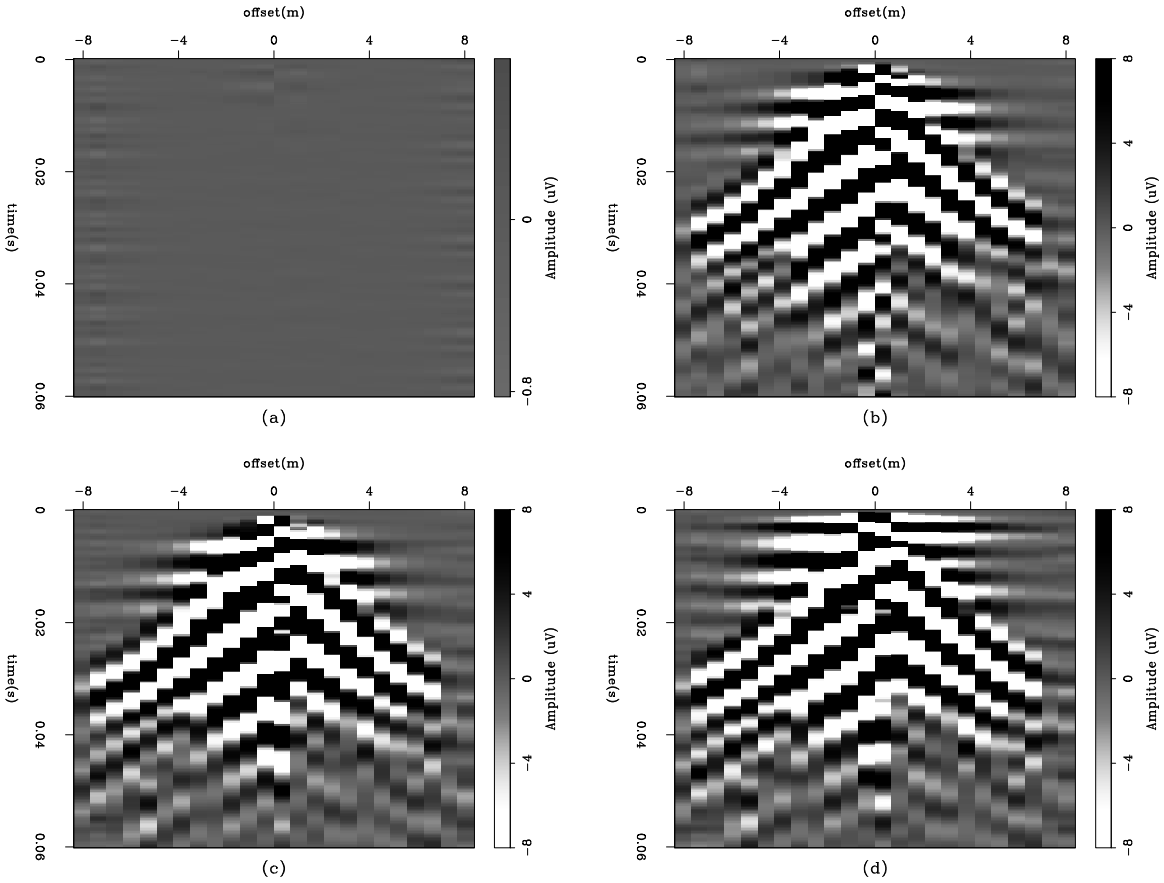

Figure 2: Electroseismic shot gathers collected at the vineyard field site testing various source options. a) stack of manual triggers. Note absence of any coherent arrivals. b) Wooden fence post on plastic hammer plate. Note flat direct field arrivals and dipping coseismic energy. c) Metal sledgehammer on plastic hammer plate. Gather appears very similar to that in b). d) Metal sledge on aluminum hammer plate. Note addition of flat Lorentz field energy in the upper ∼0.01 s. shaines1-pmv_series [CR,M]

The series of gathers shown in Figure 2 was collected at the vineyard field site described in detail by Haines and Guitton (2002). The site is a small meadow at a vineyard in St. Helena, CA. The soil is fairly homogeneous and clay-rich, and extends to a depth of at least 3m. Although the homogeneity has been disrupted by the construction of two sand-filled trenches, the data in Figure 2 were collected away from the trenches such that they should have no impact on the displayed data. The data were collected with a source point in the center of an array of 24 electrode pairs at a spacing of 0.7m. The distance across each pair of electrodes (the dipole width) is 1.05m. All gathers are the result of stacking individual impacts of the source (frequently a sledgehammer) on a metal or plastic hammer plate. Generally 25 or 30 impacts were recorded separately and then those that do not show any strong electrical noise in the time window of interest are stacked to produce the gathers shown. Final gathers are generally the result of stacking between 10 and 25 individual impacts.

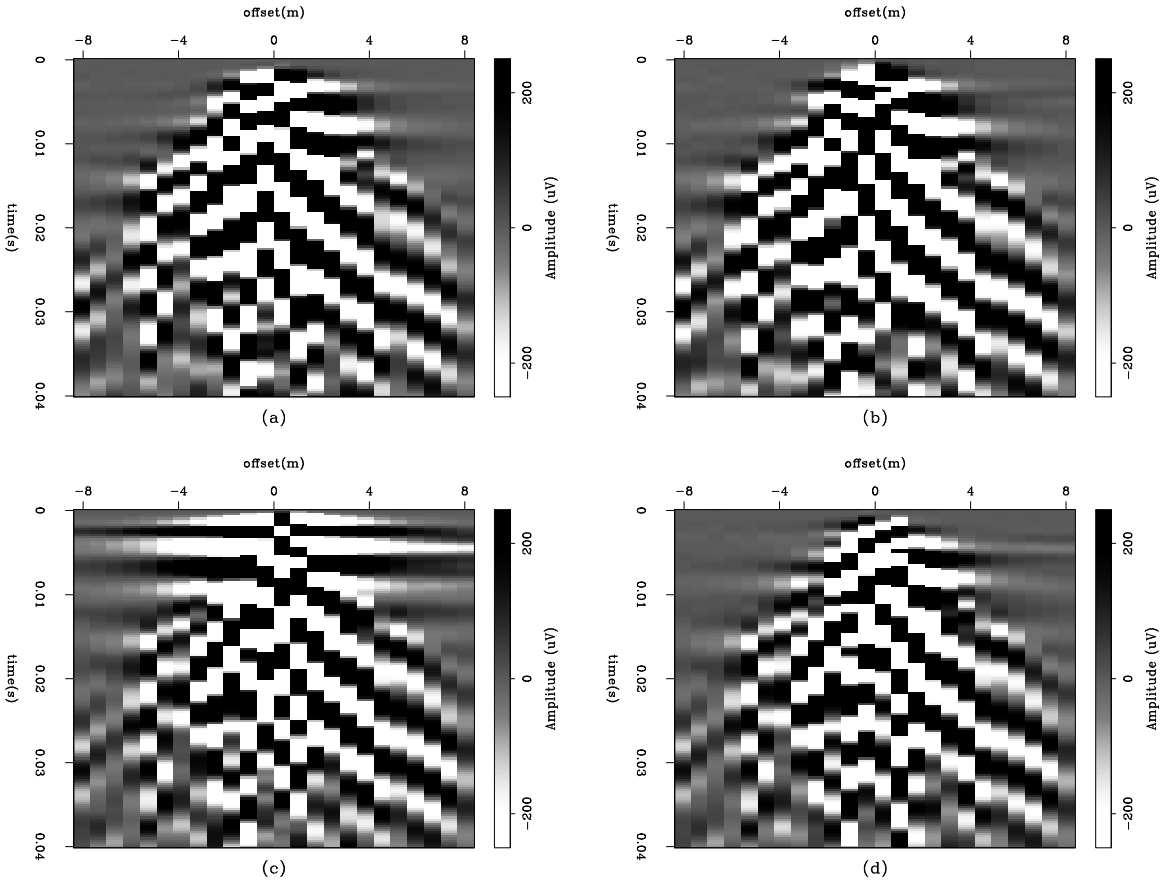

Figure 3: Electroseismic data from the Thompson tree farm with various source types. a) Wooden fence post on plastic hammer plate. Note flat direct field energy and dipping coseismic energy. b) Metal sledgehammer on plastic plate. c) Metal sledge on aluminum plate. Note addition of flat Lorentz field energy. d) Metal sledge on aluminum plate BUT plate is insulated from the earth. Note that Lorentz field energy is absent. shaines1-gat_series [ER,M]

The simplest possible data collection example is carried out by manually triggering the recording seismograph. Figure 2a shows data collected by hitting the trigger switch against a stationary object. Thus the data represent electrical background noise and the lack of any coherent energy demonstrates that the trigger mechanism produces no electrical noise. Next we add a level of complexity by putting seismic energy into the ground, but with no moving metal objects. Figure 2b shows data collected using the impact of a wooden source (a fence post) on a plastic hammer plate. We now see the expected dipping coseismic energy (with seismic moveout). We also observe flat (no moveout) energy in the upper $\sim$17 ms of the record. This energy appears to show the amplitude pattern of a dipole and reversed polarity on opposite sides of the shot point. If the site geology included any shallow interfaces, we might conclude that this flat energy was the electroseismic interface response. However, it does not, so we interpret this energy as the electroseismic direct field. We will re-visit this interpretation in the next section. We add another level of complexity by using a metal sledgehammer on the plastic hammer plate (Figure 2c) and observe that the result is very similar to that of Figure 2b.

Thus we can conclude that the moving metal hammer head does not create a noticeable electric field. We move one step further by employing a metal hammer plate (an aluminum cylinder ∼0.2m long and ∼0.15m in diameter, positioned with its axis horizontal). We now observe (Figure 2d) an additional form of flat energy in the upper ∼10 ms of the record. It shows no moveout, and an amplitude pattern suggestive of a dipole. But unlike the interface response and the direct field, this energy shows the same polarity on the two sides of the shot point. Thus we conclude that this energy is due to a horizontal electric dipole oriented along the electrode transect line. The Lorentz field (Equation 3) offers the most likely explanation for the observed energy. The motion ($\mathbf{v}$) of the conductive hammer plate in the Earth's magnetic field ($\mathbf{B}$) produces an electric field $\mathbf{E}$. We further examine this field later in this contribution.

In order to gain more certainty in our interpretations, we examine data from a separate field site. The data in Figure 3 were collected at the Thompson tree farm in the Santa Cruz mountains of California. The site is remote from cultural noise (both electrical and seismic) and has a subsurface geology that we consider to be free of any distinct interfaces in the upper few meters. Figure 3a shows a gather collected using a wooden source on a plastic hammer plate with dipping coseismic energy and (faint) flat direct field energy clearly visible. The gather in Figure 3b looks very similar, and was collected using a metal sledgehammer on the plastic hammer plate. Figure 3c shows data collected with a metal hammer on the aluminum hammer plate, and it shows the strong Lorentz electric field as well as the dipping coseismic energy. The gather in Figure 3d was also collected with the hammer on the aluminum hammer plate, but in this case the plate was insulated from the earth by a thin layer of wool material. The Lorentz field is not observed, demonstrating the need for electrical contact between the metal hammer plate and the earth for observation of this field. Thus a metal hammer plate may be used for electroseismic work if it is insulated from the earth.

A MORE DETAILED ANALYSIS

Electroseismic direct field

In order to characterize both the direct field and the Lorentz field, we conducted a series of experiments involving the recording of various sources with electrode pairs deployed in a circular geometry. The electrode array was spaced evenly around a circle of radius 4.3m in a homogeneous part of the vineyard meadow, with 12 electrode pairs oriented radially and 12 oriented tangentially. Thus tangential and radial pairs of electrodes were co-located at 30 degree intervals around the circle. The source point is in the center of the circle for all shot gathers. Figure 4a shows the radial traces of a shot gather collected with a sledgehammer striking the plastic plate. Based on arrival times from the data shown in Figure 2, we can interpret the strong coherent arrival at 0.02 seconds as the coseismic energy, and the weaker arrival at 0.01 seconds as the direct field. These arrivals do not appear in the tangential part of the same shot gather (Figure 4b), as is to be expected for a vertical dipole (the direct field) and radially propagating seismic energy (the coseismic arrival). Further confirmation of our interpretation of the 0.02 second arrival as coseismic energy is provided by the corresponding radial horizontal geophone data shown in Figure 4c, where we see that the first seismic arrival

closely matches the interpreted coseismic arrival in Figure 4b. The lack of any energy at ∼0.01 seconds in Figure 4c supports our interpretation of the 0.01 second energy in Figure 4a as the direct field, or at least as an electroseismic arrival. As is to be expected, the tangential geophone data (Figure 4d) do not show coherent arrivals.

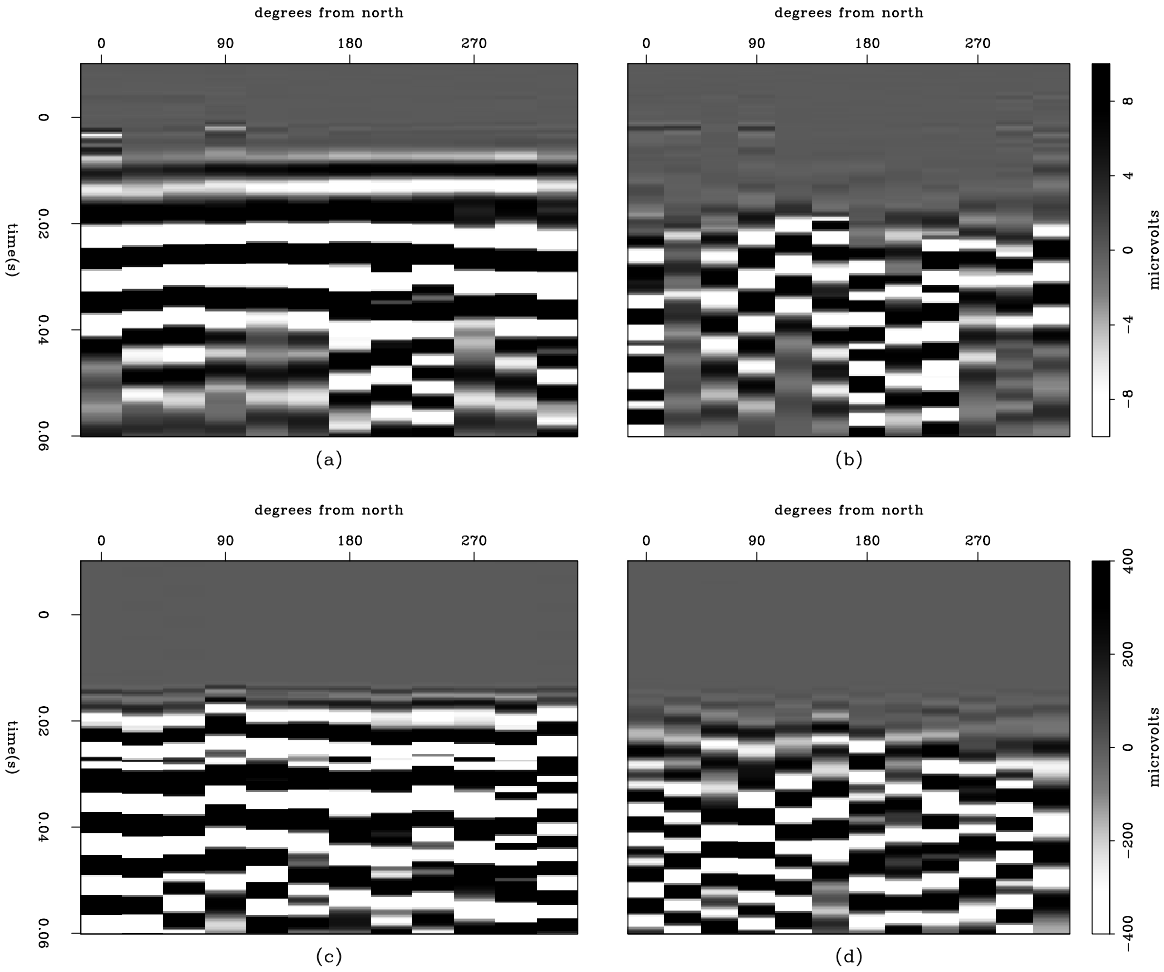

Figure 4: Stacked shot gathers recorded by the circular electrode array described in the text. a) Radial component of electric field created by the impact of a sledgehammer on a plastic hammer plate. Note coherent direct field arrival at ∼0.01 sec and coseismic arrival at ∼0.02 sec. b) Tangential component of the same shot gather (hammer on plastic plate) with no coherent arrivals. c) Radial component of horizontal geophone data, with first seismic arrival at ∼0.02 sec, corresponding with coseismic arrival in a). d) Tangential component of geophone data, with no clear coherent arrivals. shaines1-circle1 [ER,M]

The fact that the direct field energy in Figure 4a shows (approximately) constant amplitudes around the circle is consistent with the interpretation that this energy is due to a vertical dipole. The deviations from constant amplitude are likely caused by imperfect electrode coupling. We can constrain the size and location of this dipole by considering the amplitude pattern of the in-line shot record shown in Figure 2c. Figure 5a shows the same data, but with a lower-frequency bandpass filter (so as to better represent the full direct field, which can be

clearly seen as a single strong arrival at ∼0.005 seconds). The amplitude of the maximum of this arrival is plotted as dots in Figure 5b. Using the equation for the amplitude pattern of a dipole

$$V(x,z) = \frac{qd}{4\pi\epsilon_0}\,\frac{z}{(x^2+y^2)^{3/2}}, \tag{4}$$

(where q is the charge and d is the separation between poles) we model amplitudes corresponding with a disk of dipoles with radius 0.8m and located at a distance of 0.8m from the electrode receiver line, plotted as a solid line in Figure 5b. The fit of this model to the data broadly indicates that the direct field is produced within a volume of earth of radius ∼0.8m. The absolute magnitude of the modeled dipole is entirely arbitrary; it is simply scaled to match the real data. The numerous variables that contribute to the real magnitude are too complex to permit exact modeling.

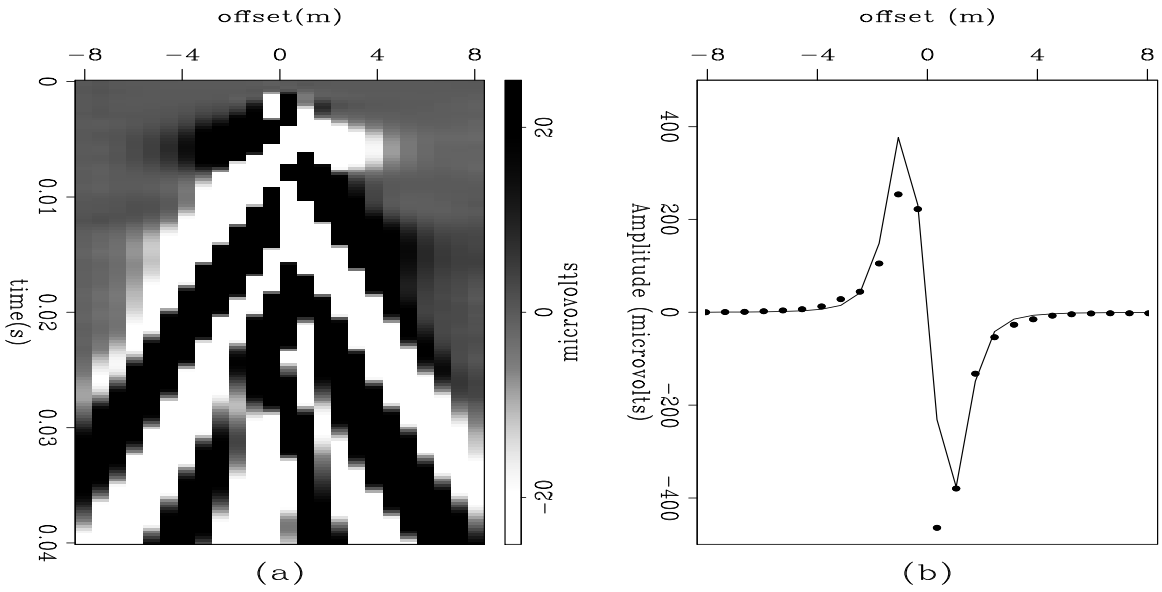

Figure 5: Direct field amplitudes. (a) Shot gather from Figure 2c, shown with bandpass filter 20 to 800 Hz. (b) Amplitude pattern for the direct field arrival at ∼0.005 seconds of gather in (a) plotted as dots, and modeled amplitudes as a solid line. Modeled amplitudes correspond with a disk of electric dipoles of radius 0.8m centered at 0.8m away from the electrode array. shaines1-direct_amps [ER]

Electric field of the metal hammer plate

One important observation about the Lorentz field is that its polarity reverses between sequential hammer strikes, such that approximately half of the raw hammer gathers show one polarity, and the other half show the opposite polarity. The stacks shown in Figures 2d and 3c are made from shot gathers selected on the basis of the polarity of the Lorentz field. The other

gathers would produce a stack with a Lorentz field arrival with opposite polarity. A stack of all of the shot gathers would show very little Lorentz energy as it tends to stack out.

Data collected by the circular electrode array using the sledgehammer on the aluminum hammer plate are shown in Figure 6. Figure 6a and b are the radial and tangential parts of a partial stack of hammer strikes, and 6c and d are the radial and tangential parts of a stack of the other hammer strikes. These two sets of impacts were selected from the individual hammer strike gathers based on the presence and polarity of the events that appear at a time of $\sim$0.001 seconds at certain radial positions (90-180° and 240-330°) in the radial component and 90° out of phase (0-90° and 180-270°) in the tangential component. Note that the polarity of these arrivals is reversed between the two stacks (Figure 6a and b, versus Figure 6c and d).

The radial pattern of these arrivals suggests that they are due to a horizontal electric dipole oriented a few tens of degrees west of north, with the orientation of the dipole reversed between the two sets of gathers. Because the field occurs only for hammer impacts on a metal plate, we assume that it is caused by the metal plate, and that it is the Lorentz field (Equation 3). Because the orientation of the dipole reverses phase between sequential hammer impacts, we must assume that it is caused by a component of $\mathbf{v} \times \mathbf{B}$ that can reverse from one strike to the next. The earth's magnetic field $\mathbf{B}$ is essentially constant (oriented toward magnetic north, and inclined at an angle of $\sim$60° from horizontal), so we must look to $\mathbf{v}$ for this reversal. Although the dominant component of $\mathbf{v}$ is vertical, there is also a small horizontal component due to the imperfect impact of the hammer on the rounded top of the aluminum block. For the case of the in-line data (Figure 2d and Figure 3c), the aluminum cylinder is oriented along the electrode receiver line, and thus the hammer strikes will tend to cause horizontal motion perpendicular to the line. If we take the cross product of this velocity with the vertical component of $\mathbf{B}$, we get a horizontal electric field $\mathbf{E}$ oriented along the electrode line, just as we observe. The orientation of the horizontal component of $\mathbf{v}$ will vary from strike to strike, but will generally be perpendicular to the electrode transect line, in one of two primary polarities. We conclude that the observed electric field is due to the horizontal component of the hammer plate velocity crossed with the vertical component of the earth's magnetic field.

Next we extract the amplitudes of the observed arrivals and compare them with modeled amplitudes. Figure 7a shows the amplitude of the Lorentz field event shown in Figure 6a and b, while Figure 7b shows the amplitude of the Lorentz in Figure 6c and d. The radial component is plotted as a solid line and the tangential component as a dashed line. The amplitude in Figure 7a corresponds with the third of the three phases of the Lorentz field arrival in Figure 6a (0.0042 to 0.0065 seconds) while the amplitude in Figure 7b was extracted from the second of the three main phases of the Lorentz event in Figure 6b (0.0025 to 0.0045 seconds), thus the two amplitude patterns are in-phase while the two displayed Lorentz events are 180° out-of-phase. We use Equation (4) to model a horizontal dipole at the source point, and find that a best fit is achieved with a dipole oriented $\sim$50° west of north. This alignment corresponds with the alignment of the hammer plate and the person swinging the hammer, not with magnetic north, confirming our interpretation that the horizontal $\mathbf{v}$ of the hammer plate and the vertical component of the earth's field $\mathbf{B}$ are responsible for the Lorentz field. The horizontal component of $\mathbf{B}$ does not seem to play a role in the creation of this field.

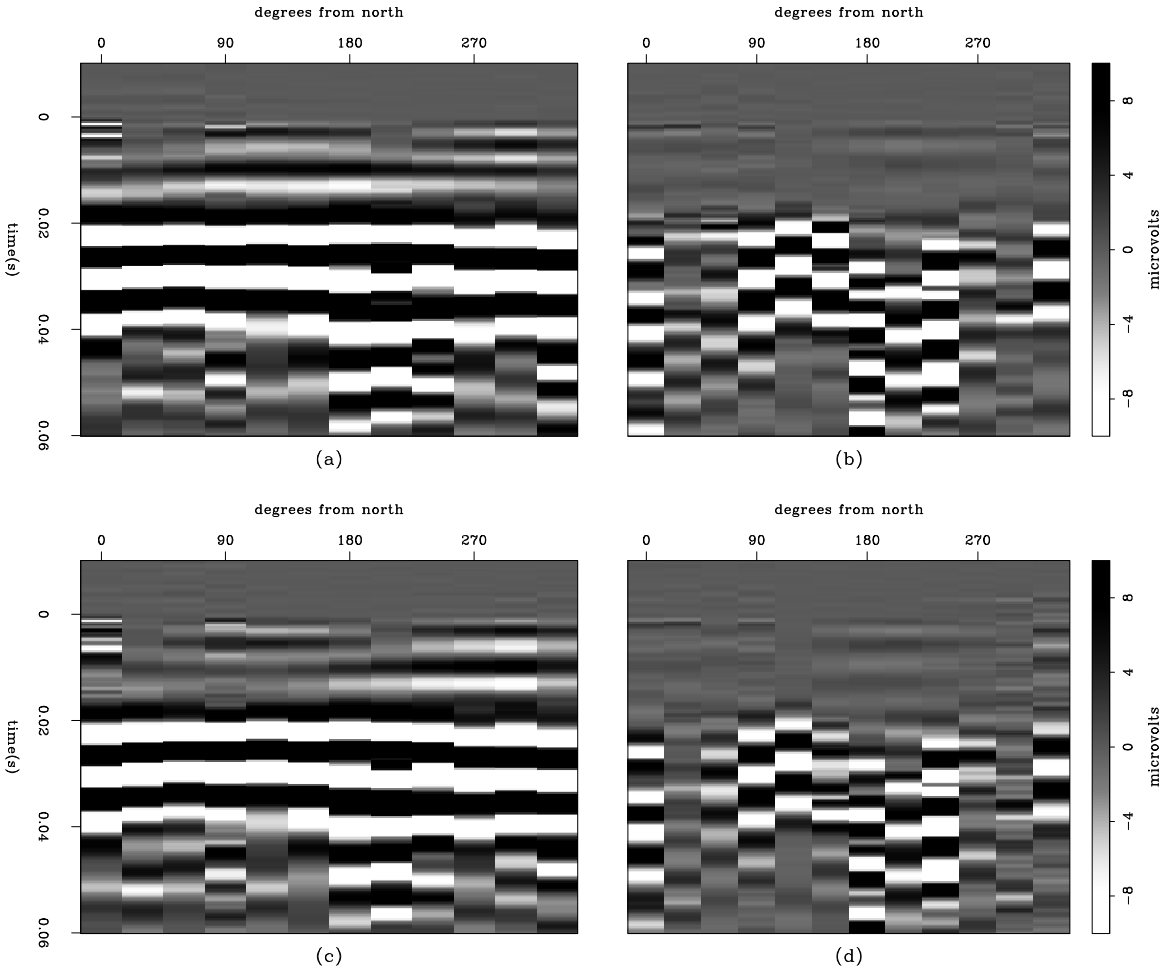

Figure 6: Electroseismic data collected with a sledgehammer on the aluminum hammer plate and recorded by the circular electrode array. Lorentz energy can be seen at ∼0.001 s in each gather. a) Radial component of stack of selected hammer strikes. Note Lorentz energy at ∼0.001 s at certain radial positions. b) Tangential component of the same stacked gathers, with faint Lorentz energy at ∼0.001 s at positions orthogonal to the energy in a). c) Radial component of a stack of other shot gathers, with similar energy at ∼0.001 s but with reversed polarity relative to a). d) Tangential component of stack of the same gathers as c), again showing Lorentz energy at positions orthogonal to the energy in c). shaines1-circle2 [CR,M]

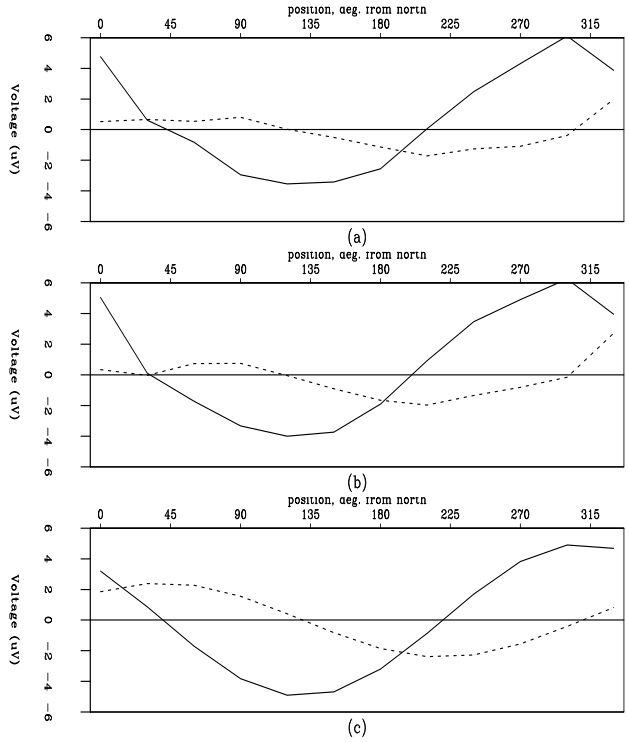

Figure 7: Comparison between real and modeled Lorentz energy as a function of radial position. a) Amplitude (solid=radial, dashed=tangential) patterns extracted from the stacks in Figure 6a and b. b) Amplitudes extracted from stacks in Figure 6c and d. c) Amplitude pattern modeled for a dipole oriented 50° west of north. shaines1-circ_amps [CR]

We can gain further knowledge about the Lorentz field by extracting amplitudes from the in-line data (Figure 2d). Figure 8a and c show stacks of two different sets of impacts collected with the metal hammer plate processed with a broad bandpass filter (20 to 800 Hz); the data in Figure 8a is the same stack as in Figure 2d. Both of these data plots show a strong flat arrival at about 0.002 seconds which we interpret as the Lorentz field, followed by another flat event with reversed polarity on opposite sides of the shot point. This second arrival is the direct field. Amplitudes extracted from these stacks for the Lorentz field are show in Figure 8b and d as dots. Modeled amplitudes for a horizontal electric dipole matching the hammer plate (charge separation of 0.2m between ends of the dipole, lateral offset of 0.25m from the receiver line) are plotted as solid lines. Only the magnitude and polarity of the modeled dipole is varied between the two plots. The central two traces show polarity opposite that of the rest of the Lorentz field because they are located along the horizontal dipole and so are measuring the field off of its main axis, where the field is opposite to the direction of the dipole.

DISCUSSION

We have identified and described two different forms of electrical energy that may be created by the standard hammer-on-metal-plate seismic source option. The motion of the metal plate itself creates an electric field, which we refer to as the Lorentz field, due to the physics implied by Equation (3). The second effect is electrokinetic in origin, and is termed the “direct field”. It is the field of the electrical charge separation caused by the asymmetrical pressure gradient created at an impact source (such as a sledgehammer).

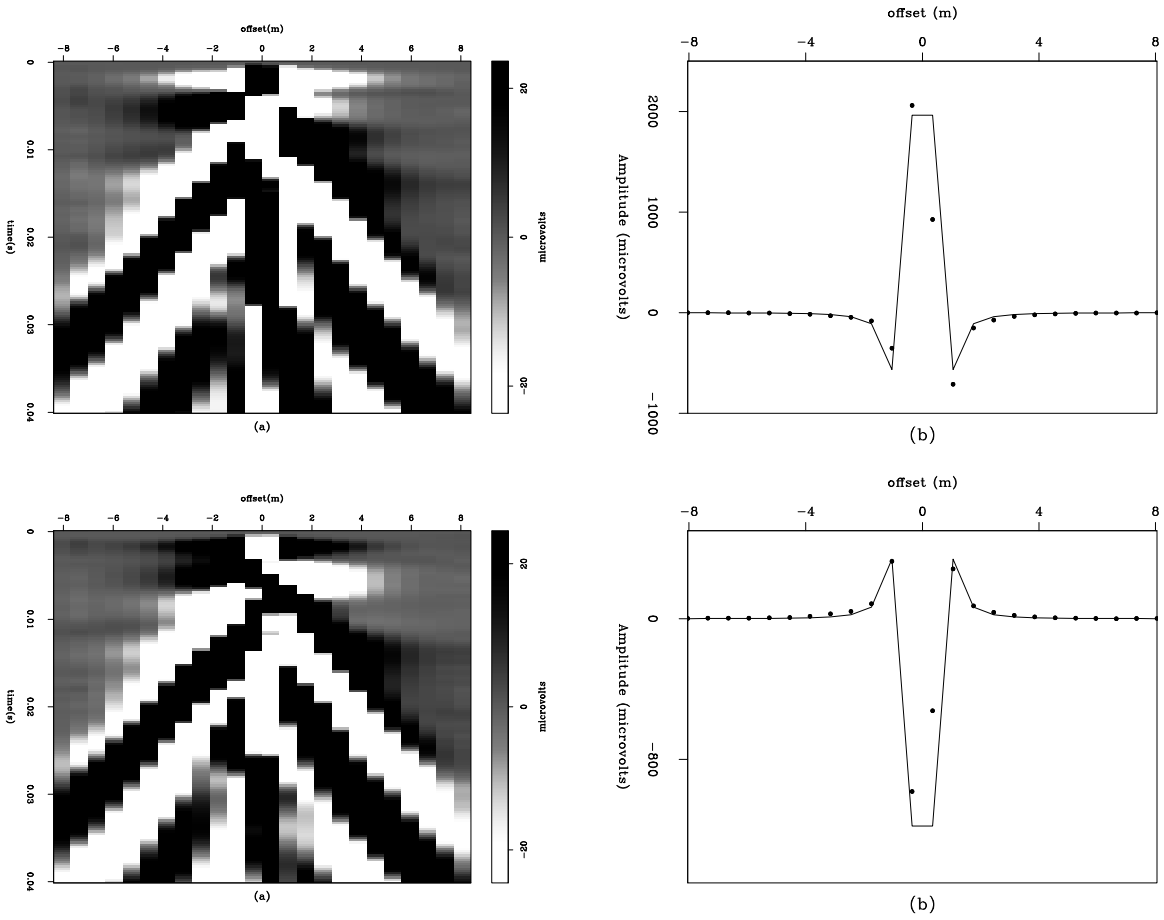

Figure 8: In-line data showing the Lorentz field at ∼0.001 s, the direct field at ∼0.005 s, and modeled and real amplitudes. a) Stacked data shown in Figure 2d, but with lower-frequency bandpass filter (20 to 800 Hz). b) Real amplitudes (dots) of Lorentz field arrival of data in a), and modeled amplitudes (solid line) corresponding with the metal hammer plate acting as an electric dipole oriented along the electrode array. c) Stack of other selected shot gathers (those with Lorentz field arrival opposite in polarity to stack in part a). d) Real (dots) and modeled (solid line) amplitudes for metal plate as a horizontal dipole as predicted by the Lorentz equation. shaines1-metal_amps [CR]

The Lorentz field is unlikely to prove useful, and so is a noise source to be avoided. Fortunately this can easily be achieved with the use of a non-metal hammer plate, or insulation between a metal plate and the earth.

The direct field could potentially be used to measure physical properties of the region where it exists (immediately around the source). Though not terribly interesting at the surface, measurement of the direct field in a down-hole setting could prove useful.

ACKNOWLEDGMENTS

We are very grateful to Jim and Carolyn Pride for the use of their land (the vineyard site) and for their ongoing generosity. We are also very grateful to George and Anita Thompson for the use of their property, and to George for his continued support and general guidance. Steve Pride has played an integral role throughout this project, and made important contributions to this paper. Biondo Biondi, Simon Klemperer, Jerry Harris, and Art Thompson have all made major contributions to this research project as a whole, and have provided valuable guidance throughout. The data presented in this paper were made possible by the sweat of those who swung the hammer: Mike Beman, Morgan Brown and Phil Resor. We also greatly appreciate the efforts of the many others who have swung the hammer as part of other data collection efforts. Financial support has been provided by The American Chemical Society's Petroleum Research Fund, an Achievement Rewards for College Scientists fellowship, the Stanford Exploration Project, the American Association of Petroleum Geologists Grants-in-Aid program, the Geological Society of America's graduate student fellowship program, the Colorado Geological Survey, and the Stanford Earth Sciences McGee Fund.

REFERENCES

Butler, K. E., Russell, R. D., Kepic, A. W., and Maxwell, M., 1996, Measurement of the seismoelectric response from a shallow boundary: Geophysics, **61**, no. 06, 1769–1778.

Garambois, S., and Dietrichz, M., 2001, Seismoelectric wave conversions in porous media: Field measurements and transfer function analysis: Geophysics, **66**, no. 5, 1417–1430.

Haines, S., and Guitton, A., 2002, Removal of coherent noise from electroseismic data: SEP–**111**, 183–201.

Haines, S., Pride, S., Klemperer, S., and Biondi, B., 2004, Development of electroseismic experimental methods: Symposium on the Application of Geophysics to Engineering and Environmental Problems, Environmental and Engineering Geophysical Society, procedings, 1490–1503.

Pride, S. R., and Haartsen, M. W., 1996, Electroseismic wave properties: J. Acoust. Soc. Am., **100**, no. 3, 1301–1315.